

See discussions, stats, and author profiles for this publication at: <https://www.researchgate.net/publication/233863380>

# Effect of the Zn content in the structural and magnetic properties of $\text{Zn}_x\text{Mg}_{1-x}\text{Fe}_2\text{O}_4$ mixed ferrites monitored by Raman and Mössbauer spectroscopies

Article in Journal of Applied Physics · January 2010

CITATIONS

14

READS

141

7 authors, including:



**Sebastião W da Silva**

University of Brasília

155 PUBLICATIONS 2,553 CITATIONS

[SEE PROFILE](#)



**Fabio Nakagomi**

Universidade Federal de Itajubá (UNIFEI)

20 PUBLICATIONS 426 CITATIONS

[SEE PROFILE](#)



**Adolfo Franco Jr**

Universidade Federal de Goiás

76 PUBLICATIONS 1,931 CITATIONS

[SEE PROFILE](#)



**Vijayendra Kumar Garg**

University of Brasília

242 PUBLICATIONS 3,276 CITATIONS

[SEE PROFILE](#)

Some of the authors of this publication are also working on these related projects:



Indium doped  $\text{LiFePO}_4$  [View project](#)



Hafnium [View project](#)

# Effect of the Zn content in the structural and magnetic properties of $\text{Zn}_x\text{Mg}_{1-x}\text{Fe}_2\text{O}_4$ mixed ferrites monitored by Raman and Mössbauer spectroscopies

S. W. da Silva,<sup>1</sup> F. Nakagomi,<sup>1,a)</sup> M. S. Silva,<sup>2</sup> A. Franco, Jr.,<sup>2</sup> V. K. Garg,<sup>1</sup> A. C. Oliveira,<sup>1</sup> and P. C. Morais<sup>1</sup>

<sup>1</sup>*Instituto de Física, Universidade de Brasília, Núcleo de Física Aplicada, Brasília DF 70910-900, Brazil*

<sup>2</sup>*Instituto de Física, Universidade Federal de Goiás, C.P. 131, Goiânia GO 74001-970, Brazil*

(Presented 21 January 2010; received 30 October 2009; accepted 18 January 2010; published online 19 April 2010)

Samples of  $\text{Zn}_x\text{Mg}_{1-x}\text{Fe}_2\text{O}_4$  ( $0 \leq x \leq 1$ ) synthesized by the combustion reaction method were investigated by x-ray diffraction, Mössbauer spectroscopy, and Raman spectroscopy. All the samples are found to have a cubic spinel structure and the lattice parameter increases linearly with increasing Zn-content ( $x$ ). The Mössbauer data showed that the replacement of  $\text{Mg}^{2+}$  ions for  $\text{Zn}^{2+}$  ions changes substantially the hyperfine parameter. Moreover, it was verified the presence of  $\text{Fe}^{3+}$  ions both in  $A$  and  $B$  sites. The Raman spectra showed five predicted Raman bands for the spinel structure and it was observed the splitting of the  $A_{1g}$  Raman mode into tree branches, where each one have been attributed to peaks belonging to each ion (Zn, Mg, and Fe) in the tetrahedral positions. © 2010 American Institute of Physics. [doi:10.1063/1.3350903]

## I. INTRODUCTION

The magnetic properties of ferrites are strongly dependent on the cation distributions. Spinel magnetic oxides can be represented by  $M\text{Fe}_2\text{O}_4$  formula ( $M$  is a divalent metal ion and Fe is a trivalent iron ion). Occupation of the tetrahedral sites ( $A$  sites) entirely with divalent cations produce a normal spinel structure, while occupation of the octahedral sites ( $B$  sites) with divalent cations yield an inverse spinel structure. In bulk form,  $\text{ZnFe}_2\text{O}_4$  is usually assumed to be a completely normal spinel with all  $\text{Fe}^{3+}$  ions on  $B$  sites and all  $\text{Zn}^{2+}$  ions on  $A$  sites. On the other hand, it has been showed that in the  $\text{MgFe}_2\text{O}_4$  ferrite, the site preference of the divalent ions leads to a predominantly inverse structure with  $\text{Mg}^{2+}$  ions mainly on  $B$  sites and  $\text{Fe}^{3+}$  ions distributed almost equally among  $A$  and  $B$  sites.<sup>1</sup> Ferrite spinels may also contain mixture of two divalent metal ions such as  $\text{Zn}_x\text{Mg}_{1-x}\text{Fe}_2\text{O}_4$  in which  $\text{Mg}^{2+}$  and  $\text{Zn}^{2+}$  ratio may be varied. In this case, it is expected that zinc ions replace magnesium ions, between  $x=0$  and 1,  $\text{Zn}^{2+}$  ions appear to enter preferentially tetrahedral positions while the  $\text{Fe}^{3+}$  ions should be displaced from these sites for the octahedral sites. However, in spite of the fact that for nanocrystalline systems such behavior is not always observed and there are few studies on this subject.<sup>2,3</sup> In present work, the effect of  $\text{Zn}^{2+}$  nonmagnetic ions on structural and magnetic properties of cubic  $\text{Zn}_x\text{Mg}_{1-x}\text{Fe}_2\text{O}_4$  ( $0 \leq x \leq 1$ ) nanoparticles have been investigated by means of x-ray diffraction (XRD), Mössbauer spectroscopy, and Raman spectroscopy.

## II. EXPERIMENTS

A series of mixed magnesium-zinc ferrite with the general formula  $\text{Zn}_x\text{Mg}_{1-x}\text{Fe}_2\text{O}_4$ , with  $0.0 \leq x \leq 1.0$  was synthe-

sized by the combustion reaction method<sup>4</sup> without subsequent calcination steps. All reagents, iron nitrate  $\text{Fe}(\text{NO}_3)_3 \cdot 9\text{H}_2\text{O}$ , zinc nitrate  $\text{Zn}(\text{NO}_3)_2 \cdot 6\text{H}_2\text{O}$ , magnesium nitrate  $\text{Mg}(\text{NO}_3)_2 \cdot 6\text{H}_2\text{O}$ , and urea  $\text{CO}(\text{NH}_2)_2$  as fuel, were analytical grade and manipulated in air without the protection of nitrogen or inert. The chemical composition (total zinc and magnesium contents) of all ferrite samples was determinate by atomic absorption spectrophotometry using the commercial Perkin-Elmer 5000 system. The calculated composition is in good agreement with the core chemical composition determinate by atomic spectroscopy (see Table I). The as-prepared powder were characterized by XRD using a Shimadzu diffractometer (model 6000) with  $\text{Cu-K}_\alpha$  radiation ( $\lambda=1.5418 \text{ \AA}$ ) in a wide range of Bragg angles ( $15^\circ < 2\theta < 80^\circ$ ) with a scanning rate of  $2^\circ/\text{min}$  at room temperature. Liquid nitrogen-temperature Mössbauer spectra of the as-produced samples were recorded in the transmission geometry using the  $^{57}\text{Co}$  source in Rh matrix. The system velocity was calibrated with a thin iron foil whereas the spectra were

TABLE I. The calculated composition, based on the proportions of the starting materials, and chemical composition determinate by atomic spectroscopy.

Calculated $\text{Zn}_x\text{Mg}_{1-x}\text{Fe}_2\text{O}_4$	Determined	
	$x$ (Zn)	$(1-x)$ (Mg)
0.0	0.000	0.999
0.2	0.192	0.808
0.4	0.390	0.610
0.5	0.487	0.513
0.6	0.617	0.383
0.7	0.699	0.300
0.8	0.812	0.188
1.0	0.998	0.000

<sup>a)</sup>Electronic mail: nakagomi@unb.br.

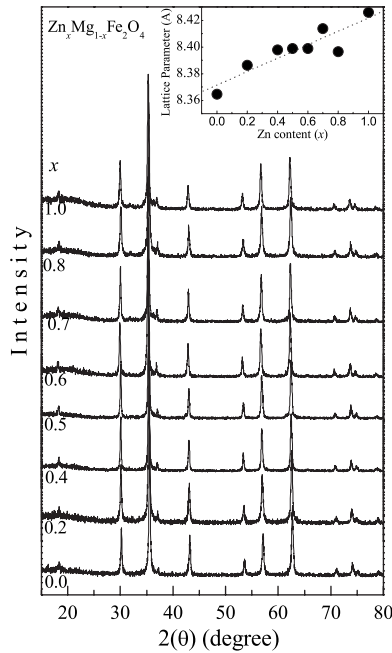


FIG. 1. XRD patterns of  $\text{Zn}_x\text{Mg}_{1-x}\text{Fe}_2\text{O}_4$  ( $0 \leq x \leq 1$ ) samples. The inset shows a plot of the deduced lattice parameter as a function of  $x$ .

least-square fitted to a combination of Lorentzian-like lines. The Raman system used to record the spectra of the samples was a commercial triple spectrometer (Jobin Yvon Model T64000) equipped with a charge-coupled device detector. The 514 nm line from an argon-ion laser was used to illuminate the samples at an optical power around 0.2 mW. All Raman measurements were performed at room temperature.

### III. RESULTS AND DISCUSSION

Figure 1 shows all XRD patterns of the spinel ferrite prepared by combustion reaction method at room temperature. XRD patterns revealed that all specimens exhibited sharp and intense peaks that correspond to the cubic inverse spinel structure of  $\text{MgFe}_2\text{O}_4$ .<sup>5</sup> The absence of extra reflections in the diffraction patterns ensures the phase purity. The mean particle sizes were calculated from x-ray line broadening of the (311) diffraction peak using Scherrer equation.<sup>6</sup> The mean particle diameter is nearly the same for all specimens; being ca. 40 and 42 nm for  $x=0.0$  and  $x=1.0$ , respectively. The XRD data show that the lattice parameter of cubic cell increases linearly with increasing Zn content ( $x$ ) following Vegard's law approximately,<sup>7</sup> see the inset on Fig. 1.

All synthesized  $\text{Zn}_x\text{Mg}_{1-x}\text{Fe}_2\text{O}_4$  samples reported in this study were examined by Mössbauer spectroscopy at 77 K, as shown in Fig. 2. At low Zn content ( $0 \leq x \leq 0.4$ ) the Mössbauer spectra was analyzed by using the assumption of Lorentzian line shapes and resolved into two subspectra: one corresponding to A site Fe ions in tetrahedral sites and the other to B site Fe ion in octahedral sites. At intermediate Zn content, the Mössbauer spectra are broader and this can be explained considering the breaking of local magnetic ordering due to increase in Zn content. For samples of  $x=0.8$  and 1.0 the Mössbauer spectra exhibits a doublet, as expected for a paramagnetic phase.

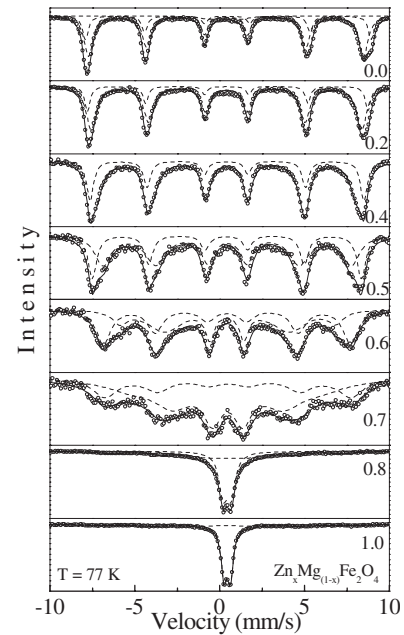


FIG. 2. Mössbauer spectra of  $\text{Zn}_x\text{Mg}_{1-x}\text{Fe}_2\text{O}_4$  ( $0 \leq x \leq 1$ ) samples recorded at 77 K.

Mössbauer parameters such as relative area (I), hyperfine field (HF), isomer shift (IS), and quadrupole splitting (QS) for all samples are listed in Table II. It is observed that the isomer shift values present opposite behavior with increasing Zn content, while A site values decrease, B site values increase up to  $x=0.4$ . For  $x>0.4$ , the IS have close values. This can be explained through the bonding nature of iron in both sites. With the increasing  $x$ , the Fe population in the A site increases while in the B site, it decreases. As ionic radius values of  $\text{Fe}^{3+}$  (0.63 Å-A sites and 0.78 Å-B sites) are smaller than ionic radius values for  $\text{Zn}^{2+}$  (0.74 Å-A site and 0.88 Å-B site) and  $\text{Mg}^{2+}$  (0.71 Å-A site and 0.80 Å-B site), there is an expected increase in the orbital's overlapping of the ions in the A sites and a decrease in the B sites, resulting in IS changing.

TABLE II. Fitted Mössbauer parameters for  $\text{Zn}_x\text{Mg}_{1-x}\text{Fe}_2\text{O}_4$  ( $0 \leq x \leq 1$ ) samples recorded at 77 K.

Samples (x) Zn	Site	I (%)	HF (T)	IS (mm/s)	QS (mm/s)
0.0	A	26.7	523.5	0.473	0.058
	B	73.3	503.5	0.380	-0.016
0.2	A	20.5	513.8	0.441	0.059
	B	79.5	495.5	0.404	-0.041
0.4	A	33.1	501.6	0.430	0.041
	B	66.9	477.2	0.426	-0.099
0.5	A	35.0	492.7	0.420	0.023
	B	65.0	454.7	0.447	-0.069
0.6	A	46.7	452.6	0.422	0.020
	B	53.3	395.0	0.451	-0.121
0.7	A	46.5	450.3	0.430	-0.046
	B	53.5	350.0	0.440	-0.197
0.8	A	Dub	...	0.430	0.470
	B				
1.0	A	Dub	...	0.440	0.378
	B				

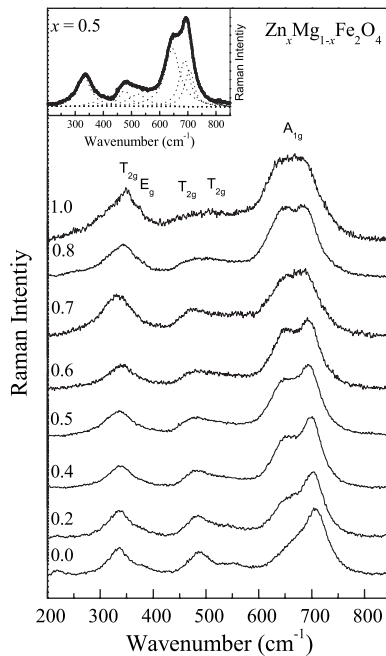


FIG. 3. The Raman spectra of  $\text{Zn}_x\text{Mg}_{1-x}\text{Fe}_2\text{O}_4$  ( $0 \leq x \leq 1$ ) samples recorded at room temperature. The inset shows the Lorentzian-like assignment to the Raman modes for the sample  $x=0.5$  in accordance with the five active optical modes.

The HF associated to both crystallographic sites (*A* and *B*) of samples  $\text{Zn}_x\text{Mg}_{1-x}\text{Fe}_2\text{O}_4$  ( $0 \leq x \leq 0.7$ ) decreases as the Zn-content increases. This can be explained considering the superexchange interaction among the neighboring metal ions in the spinel structure.<sup>8</sup> With increasing Zn content the probability of the Fe ions to find a Zn ion as nearest neighbor increases, thus HF decreases.

The relative areas of the fitted Mössbauer spectra gave the Fe ion distribution for each site. However, in the case of quaternary ferrites this information is not enough to characterize the site occupation, since it can be present in different divalent ions. In addition, for large Zn-content ( $x \geq 0.8$ ), the presence of the paramagnetic doublet makes it impossible to determine the cation distribution to each site. So, the Raman spectroscopy was employed for this study.

Figure 3 shows the room temperature Raman spectra for  $\text{Zn}_x\text{Mg}_{(1-x)}\text{Fe}_2\text{O}_4$  ( $0 \leq x \leq 1$ ) samples, recorded in the range of 200–850  $\text{cm}^{-1}$ . In this region, we have assigned the Raman modes in accordance with the five active optical modes ( $A_{1g} + E_g + 3T_{2g}$ ) characteristic of the cubic spinel  $O_h^7 (Fd\bar{3}m)$  space group; see the inset on Fig. 3. It is known from literature that Raman modes present in region 650–710  $\text{cm}^{-1}$  has  $A_{1g}$  symmetry and is related to the tetrahedral sublattice.<sup>9</sup> As

discussed in previous work<sup>10</sup> the mass difference between the three ions ( $\text{Zn}^{2+}$ ,  $\text{Mg}^{2+}$ , and  $\text{Fe}^{3+}$ ) splits the  $A_{1g}$  mode in three different energy values; the lightest ion ( $\text{Mg}^{2+}$ ) responds for the Raman mode peaking at 706  $\text{cm}^{-1}$  (for  $x=0.5$ ) whereas the heaviest one ( $\text{Zn}^{2+}$ ) responds for the 645  $\text{cm}^{-1}$  mode. Because the iron possesses an intermediate mass, we have associated the 689  $\text{cm}^{-1}$  mode for the  $\text{Fe}^{3+}$  ion in the tetrahedral sublattice (see the inset on Fig. 3). From Fig. 3, it is clearly observed in the spectra changes in the relative intensities of the peaks belonging to each ion. Following Seong *et al.*,<sup>11</sup> the integrated intensity of the Raman mode is proportional to the number of the corresponding oscillators. From this point of view, we can state that while the intensity of the  $A_{1g}(\text{Mg})$  mode decreases with the Mg-content decreases, an opposite behavior happens to  $A_{1g}(\text{Zn})$  mode when  $x$  increases. Thus it is clear that Mg, Fe, and Zn ions are present in both sites of the spinel structure.

#### IV. CONCLUSION

The influence of Zn-content on the structural and magnetic properties of  $\text{Zn}_x\text{Mg}_{1-x}\text{Fe}_2\text{O}_4$  ( $0 \leq x \leq 1$ ) quaternary spinel ferrites was investigated using Raman and Mössbauer spectroscopies. From Mössbauer data an increase was observed in the orbital's overlapping of the ions in the *A* sites and a decrease in the *B* sites, resulting in IS changing. Also, it was verified that the HF field decreases with increasing  $x$  which was due to the replacement of the ions in the spinel structure. The Raman results showed the presence of zinc, iron, and magnesium ions in tetrahedral and octahedral sites.

#### ACKNOWLEDGMENTS

The authors acknowledge the financial support from Brazilian agencies CNPq, CAPES, and FINEP.

- <sup>1</sup>V. Sepelák, D. Baabe, F. J. Litterst, and K. D. Becker, *J. Appl. Phys.* **88**, 5884 (2000).
- <sup>2</sup>S. A. Mazen, S. F. Mansour, and H. M. Zaki, *Cryst. Res. Technol.* **38**, 471 (2003).
- <sup>3</sup>C. Upadhyay, H. C. Verma, and S. Anand, *J. Appl. Phys.* **95**, 5746 (2004).
- <sup>4</sup>A. Franco, Jr., T. E. P. Alves, E. C. O. Lima, E. S. Nunes, and V. Zapf, *Appl. Phys. A: Mater. Sci. Process.* **94**, 131 (2009).
- <sup>5</sup>JCPDS Card No. 73–2211.
- <sup>6</sup>B. D. Cullity, *Elements of X-ray Diffraction* (Addison-Wesley, Reading, 1978).
- <sup>7</sup>A. R. Denton and N. W. Ashcroft, *Phys. Rev. A* **43**, 3161 (1991).
- <sup>8</sup>C. M. Srivastava, S. N. Shringi, and R. G. Srivastava, *Phys. Rev. B* **14**, 2041 (1976).
- <sup>9</sup>J. Kreisel, G. Lucazeu, and H. Vincent, *J. Solid State Chem.* **137**, 127 (1998).
- <sup>10</sup>F. Nakagomi, S. W. da Silva, V. K. Garg, A. C. de Oliveira, P. C. Morais, and A. Franco, Jr., *J. Solid State Chem.* **182**, 2423 (2009).
- <sup>11</sup>M. J. Seong, M. C. Hanna, and A. Mascarenhas, *Appl. Phys. Lett.* **79**, 3974 (2001).